**Atmospheric
Chemistry
and Physics
Discussions**

Importance of biogenic precursors to the budget of organic nitrates during BEARPEX 2009: observations of multifunctional organic nitrates by CIMS and TD-LIF

M. R. Beaver[1],[*], J. M. St. Clair[1], F. Paulot[1], K. M. Spencer[1], J. D. Crounse[1], B. W. LaFranchi[2],[**], K. E. Min[2], S. E. Pusede[2], P. J. Woolridge[2], G. W. Schade[3], C. Park[3],[***], R. C. Cohen[2], and P. O. Wennberg[1]

[1]California Institute of Technology, Pasadena, CA, USA
[2]University of California, Berkeley, CA, USA
[3]Texas A&M University, College Station, TX, USA
[*]now at: National Exposure Research Laboratory, Environmental Protection Agency, Research Triangle Park, NC, USA
[**]now at: Center for Accelerator Mass Spectrometry, Lawrence Livermore National Laboratory, Livermore, CA, USA
[***]now at: University of California, Los Angeles, CA, USA

Title Page

Abstract	Introduction
Conclusions	References
Tables	Figures

| ◄◄ | ►► |
| ◄ | ► |

| Back | Close |

Full Screen / Esc

Printer-friendly Version

Interactive Discussion

Full Screen / Esc

Abstract

Alkyl and multifunctional organic nitrates, molecules of the chemical form $RONO_2$, are products of chain terminating reactions in the tropospheric HO_x and NO_x catalytic cycles and thereby impact ozone formation locally. Many of the molecules in the class have lifetimes that are long enough that they serve as reservoir species that can be transported over large distances. If the $RONO_2$ then react to deliver NO_x to remote regions they affect ozone production rates in locations distant from the original NO_x source. While measurements of total $RONO_2$ (ΣANs) and small straight chain alkyl nitrates are routine, measurements of the specific multifunctional $RONO_2$ molecules that are believed to dominate the total have rarely been reported and never reported in coincidence with ambient ΣANs measurements. Here we describe observations obtained during the BEARPEX 2009 experiment including ΣANs and a suite of multifunctional nitrates including isoprene derived hydroxynitrates, oxidation products of those nitrates, 2-methyl-3-buten-2-ol (MBO) derived hydroxynitrates, and monoterpene nitrates. At the BEARPEX field site, the sum of the individual biogenically derived nitrates account for two-thirds of the ΣANs, confirming predictions of the importance of biogenic nitrates to the NO_y budget. Isoprene derived nitrates, transported to the site, are a much larger fraction of the ΣANs at the site than the nitrates derived from the locally emitted MBO. Evidence for additional nitrates from nocturnal chemistry of isoprene and α-pinene is presented.

1 Introduction

Nitrogen oxides affect rates of ozone production throughout the troposphere. They are emitted from soils, lightning, and natural and anthropogenic combustion, primarily as NO but also as NO_2 and HONO. In the troposphere, these compounds are oxidized to a mix of compounds including peroxynitrates (RO_2NO_2), alkyl and multifunctional nitrates ($RONO_2$), and HNO_3. The individual components of this NO_y family are transported

throughout the troposphere, where they can deposit, enriching soil N content, or undergo photochemistry releasing NO_y and contributing to enhanced production of ozone far from their source.

These molecules are formed from the reaction of organic peroxy radicals (RO_2) with NO. The major channel of this reaction forms NO_2, Reaction (R1), the photolysis of which leads to ozone formation. A minor reaction pathway of RO_2 radicals with NO forms organic nitrates, $RONO_2$, (Reaction R2).

$$RO_2 + NO \rightarrow RO + NO_2 \tag{R1}$$

$$RO_2 + NO \rightarrow RONO_2 \tag{R2}$$

The yield ($\alpha = $ R2/(R1 + R2)) of this minor, radical terminating pathway depends on the carbon chain length and structure of the VOC oxidized, and can range from a fraction of a percent for methane to 35 % for large molecules (Atkinson and Arey, 2003b). Nocturnal nitrate radical chemistry also forms organic nitrates often with large yields up to 80 % (Hallquist et al., 1999). The lifetime of these organic nitrate species with respect to deposition and further oxidation, along with the fate of the products from oxidation, control the effect of $RONO_2$ on global NO_x redistribution and local ozone formation.

The importance of alkyl nitrates to global ozone production as well as regional ozone formation has been recognized. Different chemical representations of alkyl nitrates in models, specifically isoprene nitrates, have been found to explain differences in global simulations of tropospheric ozone (Ito et al., 2007; Wu et al., 2007). Depending on the chemical mechanism used, i.e. the formation yield, lifetime, and NO_x recycling of these nitrates, ozone production behavior can vary widely (Paulot et al., 2011). Treatment of alkyl nitrates as permanent sinks for NO_x can disguise the sensitivity of ozone production to biogenic emissions such as isoprene, and causes much of the simulated global atmosphere to be VOC saturated (Wu et al., 2007). Farmer et al. (2011), using Mexico City as a case study, have recently demonstrated alkyl nitrate formation can complicate

emissions reductions aimed at decreasing urban ozone production by linking the VOC and NO_x emissions.

Isoprene nitrates are a central focus of studies investigating global ozone production since globally, isoprene (2-methyl-1,3-butadiene) emissions dwarf those of other biogenic volatile organic compounds. 440–660 $Tg\,C\,yr^{-1}$ are emitted to the atmosphere as isoprene (Guenther et al., 2006). However, regionally and locally, other VOCs such as monoterpenes and oxygenated VOCs can dominate reactivity. Isoprene has a lifetime of approximately 3 h at typical atmospheric hydroxyl radical concentrations of 1×10^6 molecules cm^{-3} (Atkinson et al., 2006). However, organic nitrates function to increase the spatial scale where relatively short-lived VOCs can impact NO_x concentrations and ozone formation. The formation of organic nitrates from biogenic VOCs couples anthropogenic NO_x emissions with naturally occuring VOC emissions.

The branching ratio between pathway (R2) and (R1) for isoprene has been studied extensively, and a range of yields for Reaction (R2) between 4.4 and 15 % have been reported (Tuazon and Atkinson, 1990; Chen et al., 1998; Chuong and Stevens, 2002; Sprengnether et al., 2002; Patchen et al., 2007; Lockwood et al., 2010; Paulot et al., 2009a). This yield has also been found to be temperature and pressure dependent (Crounse et al., 2011; Carter and Atkinson, 1989). Ambient observations over the continental US during ICARTT/INTEX-NA of alkyl nitrates attributed to isoprene are consistent with a similar range of Reaction (R2) yield (4.4 to 12 %), depending on the subsequent fate of the nitrates (Perring et al., 2009). Another analysis of this dataset using the MOZART chemical transport model suggested that a nitrate yield from isoprene of 4 % was the most consistent with the sum of ANs to ozone ratios (Horowitz et al., 2007). A deposition rate of the isoprene nitrates equal to nitric acid deposition was also necessary to explain boundary layer concentration observations.

Predictions of global ozone are very sensitive to the yield for isoprene nitrate formation. Wu et al. (2007), using the GEOS-Chem model, found a 10 % decrease in global ozone production rates by increasing the yield for isoprene nitrate formation from 4.4 % (Chen et al., 1998) to 12 % (Sprengnether et al., 2002). Currently, in GEOS-Chem,

organic nitrate formation is a terminal loss of NO_x since there is no subsequent chemistry of these compounds.

The fate of isoprene hydroxynitrates, ISOPN, has been the subject of recent research. The lifetime of ISOPN, with respect to OH and ozone is relatively short due to the presence of a double bond. For example, the E-1,4-ISOPN isomer is estimated to have a lifetime of 2.9 h (Paulot et al., 2009a) and 5.33 h (Lockwood et al., 2010) at OH = 1×10^6 molecules cm^{-3} and 40 ppb O_3, respectively. Lifetimes vary greatly amongst the possible ISOPN isomers, for the same oxidant conditions, the 1,2-IN has a lifetime of 28 h and 2.7 h with respect to OH and O_3. The oxidation of isoprene hydroxynitrates can either release NO_x as NO_2 or retain the organic nitrate functionality. Paulot et al. (2009a) have shown that approximately 50 % ± 15 % (weighted average of the 8 isomers) of the isoprene nitrates recycle NO_x upon further photooxidation by OH. Horowitz et al. (2007) found NO_x recycling of 40 % agreed with ambient observations, using a low yield of nitrates, and a fast deposition (similar to nitric acid). A fraction of isoprene hydroxynitrates retain the nitrate functionality upon oxidation by forming methyl vinyl ketone nitrate (MVKN), methacrolein nitrate (MACRN), propanone nitrate (PROPNN), and ethanal nitrate (ETHLN) (Paulot et al., 2009a). NO_x recycling levels from the ozonolysis of isoprene hydroxynitrates are unclear (Lockwood et al., 2010).

Organic nitrate yields from biogenic VOCs other than isoprene have not been studied as extensively. Alvarado et al. (1999) found a yield of 5.2 % for the dihydroxynitrate from MBO, MBON. Chan et al. (2009) report a higher yield of ∼10 % (±4 %). This molecule contains no double bond, and the lifetime with respect to OH, assuming an ambient OH concentration of 1×10^6 molecules cm^{-3} is approximately 6 days (Saunders et al., 2003). Yields and lifetimes of organic nitrates from monoterpenes such as α-pinene have also been reported. Currently, these range from 1–18 % yield (Aschmann et al., 2002; Noziere et al., 1999).

Reactions of nitrate radical with biogenic VOCs, including isoprene (Rollins et al., 2009; Perring et al., 2009), and α-pinene and β-pinene (Hallquist et al., 1999; Fry et al., 2009) are also sources of organic nitrate species. From an analysis of ICARTT field

data from the Eastern US, Horowitz et al. (2007) found half of the isoprene nitrates were formed from isoprene + NO_3 chemistry, despite a small fraction (∼6 %) of isoprene oxidized by NO_3 chemistry. Brown et al. (2009) using ambient data from flights over the Northeast US, found that 73 % of the loss of the nitrate radical was due to the oxidation of isoprene. Using the same dataset, they inferred 2–9 % of total reactive nitrogen was composed of organic nitrates formed from this reaction, using a nitrate yield of 80 % for the isoprene + NO_3 reaction (Barnes et al., 1990).

Ambient measurements of specific individual $RONO_2$ have with few exceptions (Fischer et al., 2000; Grossenbacher et al., 2001, 2004) been limited to simple alkyl nitrates. As a result of the development of thermal dissociation laser induced fluorescence (TD-LIF) by Day et al. (2002), measurement of total alkyl-nitrates (ΣANs) as a class has become routine. In this study, we use chemical ionization mass spectrometry (CIMS) measurements of organic nitrates in combination with the sum of total alkyl nitrates (ΣANs) measurements from TD-LIF to determine the absolute concentrations and speciation of organic nitrates at an urban-impacted, forested measurement site. The dataset was collected as part of the Biosphere Effects on AeRosol and Photochemistry EXperiment, BEARPEX 2009. The measurement site is locally surrounded by dominantly non-isoprene emitting pine species; however, the site receives advected isoprene and isoprene oxidation products from the oak-rich region between the measurement site and Sacramento (Dreyfus et al., 2002). One modeling study has predicted organic nitrates from isoprene and other biogenic VOCs dominate the alkyl nitrate budget at the site (Pérez et al., 2009). We report measurements of speciated first and second generation organic nitrates from isoprene and an MBO derived nitrate. We also propose chemical structures for other nitrogen-containing compounds measured at the site. Overall, these measurements confirm that the alkyl nitrate budget at this rural site is dominated by nitrates derived from biogenic VOC precursors and that $RONO_2$ is an important fraction of NO_y.

2 Experimental

2.1 Site description

The measurements presented here were obtained during the Biosphere Effects on AeRosol and Photochemistry EXperiment, BEARPEX 2009. One science goal of
5 the collaborative research campaign was to understand forest-atmosphere interactions and how the urban plume of Sacramento influences these interactions. The measurement site is located in the Western foothills of the Sierra Nevada at 38.90° N, 120.63° W, at 1315 m elevation, approximately 75 km northeast of Sacramento (Goldstein et al., 2000). The immediate vegetation is a Ponderosa pine forest plantation managed
10 by Sierra Pacific Industries. Average canopy height in 2009 was 8.7 m. The dominant summertime meteorology affecting the site is a thermally driven upslope flow that brings air from California's Central Valley into the Sierra Nevada foothills; at night, this flow reverses, and returns to the Valley (Dillon et al., 2002). The major anthropogenic inputs to the plume are from vehicular traffic in Sacramento and its surrounding sub-
15 urbs. Between Sacramento and the measurement site, there is a 30 km wide oak tree belt which contributes significant emissions of isoprene to the urban plume (Goldstein et al., 2000; Dreyfus et al., 2002). The measurement site contained two scaffolding towers used to deploy a variety of chemical and meteorological instrumentation along with sampling inlets. The Caltech CIMS instrumentation suite was located at the top of
20 the North scaffolding tower, with an inlet height of 17.8 m, approximately 9 m above the top of the forest canopy.

2.2 Instrumentation

Speciated organic nitrates were quantified using the Caltech triple quadrupole tandem chemical ionization mass spectrometer. This instrument utilizes CF_3O^- as the
25 reagent ion, and is described in detail elsewhere (St. Clair et al., 2010). This instrument was also used to measure oxidation products of isoprene during the summer

NASA ARCTAS campaign in 2008 (Paulot et al., 2009b). Briefly, ambient air was pulled through the inlet at $30\,\mathrm{m\,s^{-1}}$, then the center of this flow was sampled into the single quadrupole CIMS instrument's reduced pressure ($\sim$35 hPa) flow tube. The bypass flow was then sampled by the triple quadrupole CIMS, similar to the sampling arrangement described by St. Clair et al. (2010). The ambient flow was diluted to a 1:7 ratio with dry N_2 to lower the water vapor concentration in the flow tube.

The triple quadrupole CIMS instrument was operated alternately in two mass filtration modes: single mass spec (sMS) and tandem (MSMS) modes. When operating in sMS mode, the first quadrupole selected the m/z ratio to be observed, then the remaining two quadrupoles were used as ion guides. The data presented here were measured in sMS mode, since no known mass interferences exist. Each m/z ratio was observed for 0.5 s once approximately every 4–6 min. The remainder of the duty cycle was spent in MSMS mode. Instrumental background signals were measured at each mass, once approximately every 1.6 h, by scrubbing the analytes from ambient air using a two-stage filter containing palladium coated alumina pellets and sodium bicarbonate treated nylon wool (Spencer et al., 2011). The background signals were measured at approximately the same water vapor concentration as the ambient data. To determine ambient concentrations, an interpolation between these background signals was subtracted from the ambient signals. Also approximately every 1.6 h, ambient scans and background scans up to m/z 325 were conducted.

The CF_3O^- CIMS technique induces minimal fragmentation, therefore nitrates are observed at the m/z of the parent molecule + 85 (CF_3O^-). The lack of fragmentation aids in the determination of the molecular weight of the species, since authentic standards of the organic nitrates presented here are unavailable. Therefore, theoretical sensitivity calculations have been applied to determine concentrations. Relative sensitivities of the organic nitrates to nitric acid were assumed to be equal to the relative rates of the molecule's collision with CF_3O^-. The collision rates with CF_3O^- were calculated according to Su and Chesnavich (1982) and Garden et al. (2009). Polarizibilites and dipole moment calculations were conducted using quantum chemical

computations using the B3LYP/6-31G(d) level of theory. Comparisons of theoretical sensitivity calculations to measured sensitivities has been shown to compare well (Paulot et al., 2009b). For some analytes, the sensitivity of this technique is known to depend on water (Crounse et al., 2006; St. Clair et al., 2010). To determine the sensitivity of the nitrate clusters with the CF_3O^- reagent ion, environmental chamber experiments were performed to produce the isoprene hydroxynitrates, similar to the conditions outlined in Paulot et al. (2009a). The CIMS sampled from the sample chamber and water vapor was varied across the relevant range for this campaign, and sensitivity remained constant. Therefore, no water dependent sensitivity was applied to the ambient data. Nitrate formation yields determined from these experiments were in agreement with Paulot et al. (2009a). The estimated uncertainty for the CIMS concentrations presented here is ±40 %, dominated by the uncertainty in the theoretical predictions of sensitivity.

The signal at any *m/z* can contain an interference from the naturally occurring ^{13}C isotope signal produced from the species at the *m/z* −1 amu. The higher the number of carbon atoms in a molecule, the larger the contribution to the *m/z* signal from the ^{13}C isotope. To correct for this interference, the contribution has been removed by calculating 1.1 % * the number of carbons in the molecule that produces the *m/z* −1 ion, and removing this signal at *m/z*. We evaluated this correction method using the large ambient signal at *m/z* 159 due to hydroxyacetone. The ratio of the signal at 160 to 159 was 0.047, consistent with the expectation from the *m/z* + 1 isotopologue of hydroxyacetone cluster with the reagent ion. For the nitrates presented here, this correction was large only for the PROPNN signal, observed at *m/z* 204, due to the large ambient signal observed at *m/z* 203 (isoprene hydroxyhydroperoxide + isoprene dihydroxyepoxide) (Paulot et al., 2009a).

The sum of total alkyl nitrates, ΣANs, measurement was made by the University of California, Berkeley, using a thermal dissociation laser induced fluorescence, TD-LIF, instrument similar to that of Day et al. (2002). Briefly, the instrument measures NO_2 by LIF, and thermally dissociates other constituents of NO_y into NO_2 then measures their

contribution by the difference between channels. Specifically, ΣANs characteristically dissociate to NO_2 at temperatures greater than or equal to 380 °C. The difference in the NO_2 signal between ambient air passing through the 380 °C oven (ΣANs + ΣPNs + NO_2) and the 200 °C oven (ΣPNs + NO_2) can be attributed to ANs. The instrument is

5   calibrated periodically using an NO_2 gas standard (4.9 ± 0.2 ppm NO_2 in N_2, Praxair), and the uncertainty in the measurement is ±5 %. The measurement frequency is 5 Hz. The heated inlets for this instrument were also located on the top level of the North measurement tower.

3   Results and discussion

10   ### 3.1   Suite of organic nitrates observed

Chemical structures for the nitrates measured and presented here are shown in Fig. 1. The most abundant nitrate was the first generation isoprene hydroxynitrates; this measurement is a sum of isomers. Second generation nitrates from isoprene including PROPNN, MVKN, MACRN, and ETHLN were also observed. MVKN and MACRN are

15   isobaric, therefore, our measurement is a sum of these species. MVKN and MACRN can also form from the oxidation of MVK and MACR. MBON, a dihydroxynitrate, was also measured. Each of these species has been previously observed and identified using CIMS in laboratory experiments (Paulot et al., 2009a; Chan et al., 2009).

Time series and average diurnal profiles for each of the nitrates in Fig. 1 and ΣANs

20   are shown in Fig. 2. All data are presented using Pacific Standard Time (PST). Although isoprene is not a major local emission, the isoprene hydroxynitrate is the most abundant of the nitrates observed at the BEARPEX site. MBON was less abundant than all other organic nitrates except the two carbon ETHLN. Diurnal profiles shown in red are mean concentrations on days with maximum daytime temperatures of 26 °C and

25   higher. Blue diurnal profile is the mean concentration on days with maximum temperatures less than 26 °C. This division roughly corresponds to the noticeable increase in

nitrate concentrations observed around Julian day 195. Biogenic precursor emissions should be higher at the warmer temperatures; also, more intense photochemistry is likely at the warmer temperatures (Day et al., 2008). For the isoprene hydroxynitrates and its degradation products, the diurnal profiles look very similar to advected chemical species such as anthropogenic VOCs, CO, and nitrogen oxides (Murphy et al., 2007; Day et al., 2009; Lamanna and Goldstein, 1999). These chemical species have afternoon or evening maxima between the hours of 16 and 21. MBON peaks at noon consistent with more local VOC photochemistry. The secondary MBON peak around hour 8 is similar to observations of morning peaks in NO_x (Day et al., 2009) and biogenic VOCs (Schade et al., 2000). These morning peaks have been attributed to downward mixing of the nocturnal residual layer. The differences in the diurnal patterns of this suite of organic nitrates reflect the different VOC sources relative to the site location. Also, the observations of the second generation ETHLN and PROPNN indicate the ISOPN likely form upwind of the BEARPEX forest location and are oxidized during the transport to the site.

Ambient measurements of isoprene nitrates are rare, but have been conducted over two forested locations in Michigan and Tennessee using gas chromatography followed by pyrolytic conversion to and subsequent detection of NO_2 (Grossenbacher et al., 2004, 2001). This technique speciates the isomers of the isoprene nitrates. The two locations were characterized by vastly different concentrations of isoprene nitrates, with average, midday concentrations at the Tennessee site 5–10 times greater than observed at the Michigan forest site (mean, midday ~10 pptv). The authors explained these datasets by the differences in the photochemical age of the two different airmasses. The isoprene emissions were much closer in proximity, therefore fresher and less processed at the Michigan forest site when compared with the Tennessee site. Our measurements are generally much higher than observed at either the Michigan or Tennessee sites.

3.2 Alkyl nitrates budget

Though ΣANs have been measured at this site previously, speciation of the hydroxyni-trates has not been performed. A comparison of the speciated nitrates measured using CIMS and the ΣANs is shown in Fig. 3a.

The mean ΣANs measurement during JD 199–212 is shown as the dashed line, with the speciated organic nitrates summed in individual colors. The diurnal profile of the total alkyl nitrate meaurement also looks similar to compounds known to be transported to the site, though the maximum does occur at noon when local chemistry and emissions would be expected to be a larger contribution. When summed, the identified organic nitrates measured with the CIMS comprise two-thirds of the total alkyl nitrates at the site, averaged from noon-6pm. The fraction shown in gray is discussed below. A scatter plot of ΣANs vs. the sum of the speciated nitrates (ISOPN + PROPNN + MVKN + MACRN + MBON + ETHLN) is shown in Fig. 3b. These two measurement sets are well correlated with an R^2 of 0.85.

The influence of transport on the speciation of the alkyl nitrates can be clearly seen by comparison with predictions based on local photochemical production. The production of alkyl nitrates is calculated according to Eq. (1), where α is the branching ratio to the formation of the organic nitrate (Rosen et al., 2004; Perring et al., 2010). Data used to calculate the contributions of each VOC to alkyl nitrate production are shown in Table 1.

$$P(ANs) = \sum \alpha_i k_{OH+VOC_i}[OH][VOC_i] \tag{1}$$

VOC concentrations were measured using GC-FID, and the afternoon mean from 12:00–18:00 PST is used in this analysis. Branching ratios, α, are generally taken from MCM (v3.2) (http://mcm.leeds.ac.uk/MCM) except where noted (Saunders et al., 2003). The value of α for alkyl nitrates is dependent on the distribution of the specific alkyl nitrates present. Here, we have assumed an α of 0.15 to reflect a mixture of ISOPN and other alkyl nitrates. Daytime NO concentrations at the site were typically ~75 pptv. If the alkyl nitrates at the site are mostly affected by the local production, the

atmospheric concentrations should be reflective of the alkyl nitrate production rates. Overall, based on the VOCs measured at the site, MBO is calculated to be the largest contributor (49 %) to alkyl nitrate production, with isoprene as the second most important, contributing 41 %. However, the CIMS observations show that ISOPN (38 %) and second generation nitrates from ISOPN (21 %) are a much larger contribution to the alkyl nitrate budget than MBON (7 %). Pérez et al. (2009), using an MCM (v3.1) based Lagrangian model of the Sacramento urban plume, predicted 68 % of the alkyl nitrates at the measurement site to be lumped hydroxynitrates from the OH oxidation of ISOPN, 11 % ISOPN, and 17 % MBON. This highlights that the alkyl nitrates at the site are likely a mix of transported first and second generation isoprene nitrates as well as locally produced multifunctional nitrates such as MBON. Indeed, MBON is an even smaller component of the alkyl nitrate budget than predicted by the Lagrangian model of Pérez et al. (2009). Both the measurements and the model predict the dominance of isoprene-derived nitrates, however, the model predicts the oxidation products of isoprene nitrates to dominate over the first generation isoprene nitrates.

3.3 Possible sources of unidentified alkyl nitrates

The speciated nitrates observed by CIMS account for approximately 65 % of the total organic nitrates observed with TD-LIF at the BEARPEX site. Two avenues were explored to investigate the possible sources of other organic nitrates contributing to the TD-LIF measurement of ΣANs at the site. These include the investigation of the contributions of: (1) shorter chain, C_1–C_3, alkyl nitrates as measured during the BEARPEX 2007 campaign and C_1–C_5 alkyl nitrates as measured from an airborne platform during the NASA TC[4] campaign over the BEARPEX site in 2007, (2) unidentified, nitrogen containing mass spectral signals from our CIMS data.

Though the CIMS technique has been shown to measure two and three carbon multifunctional nitrates, the technique is not sensitive to shorter carbon chain, monofunctional alkyl nitrates such as methyl, ethyl, and propyl nitrate; it is possible some fraction of the nitrates unidentified by the CIMS are composed of these alkyl nitrates. These

compounds are derived from anthropogenic VOCs, and are formed in or near Sacramento and transported to the site. A GC-MS was used during the BEARPEX 2007 (August–October) campaign to measure C_1–C_3 alkane nitrates. The sum of these species was generally <20 pptv (J. deGouw and J. Gilman, personal communication, 2009). During TC[4], the NASA DC8 aircraft flew over the BEARPEX location (10 August 2007) before landing in Sacramento. Whole air samples were collected in-flight, and analyzed off-line using GC-FID. The aircraft was at a pressure altitude of <3.5 km when near the site, and decreased in altitude before landing in Sacramento. During this transect, the C_1–C_5 alkane nitrates peak concentration was 25 pptv, at the lowest altitude, just before landing (D. Blake, personal communication, 2011). Thus, neither of these measurements indicate small chain, alkane nitrates are a large component of the alkyl nitrate budget at or near the BEARPEX site.

Mass spectral identification of nitrogen containing compounds benefits from the odd number of valence electrons in nitrogen. Parent ions or fragments of organic compounds containing an odd number of nitrogen atoms have an odd molecular weight (McLafferty and Turecek, 1993). Thus, with the CIMS technique used here, the CF_3O^- cluster with a nitrogen containing compound has an even mass. Since dinitrates do not have an odd molecular weight, any dinitrates would not be identified using this analysis. All identified organic nitrates presented here have even m/z. As deployed during this campaign, the instrument was set to scan all m/z ratios up to m/z 325 approximately once every two hours. In Fig. 3a, gray portion, we sum the signals from the nine even m/z that carry essentially all the additional intensity from nitrogen containing compounds. In the absence of sensitivity calculations for each species, a CIMS sensitivity equal to the sensitivity for ISOPN has been applied to these signals. The summed m/z are listed in Table 2. Possible structures for four of the nine even m/z compounds are shown in Fig. 4.

Signals at m/z 230 and m/z 248 have been observed in smog chamber isoprene + NO_3 experiments (Ng et al., 2008). Since vegetative emission of isoprene is known to be light-dependent, no isoprene is emitted at night, when nitrate radical chemistry

would be expected to be active. However, isoprene emitted late in the day when photochemical oxidants are low has been found to be oxidized by the nitrate radical (Brown et al., 2009; Starn et al., 1998). Specifically, the proposed structure for *m/z* 230 is a product from isoprene + NO_3 chemistry, forming a nitrooxyperoxy radical, which upon further reaction with RO_2 or NO_3 can form the C_5-nitrooxycarbonyl. This compound, the C_5-nitrooxycarbonyl, could also result from OH-initiated oxidation of ISOPN via H-abstraction from the carbon alpha to the OH group, however, this product has not been observed to be a significant product of ISOPN photooxidation in smog chamber experiments (Paulot et al., 2009a). The structure proposed for *m/z* 248 is also a product of isoprene + NO_3 chemistry; to form this product, the nitrooxyperoxy radical reacts with HO_2 to form the C_5-nitrooxyhydroperoxide. The signal at *m/z* 248 could also result from MBO + NO_3 chemistry, however, the lifetime of MBO with respect to NO_3, for conditions relevant to the site is expected to be longer than a month (Atkinson and Arey, 2003a).

We propose a nitrooxyhydroperoxide structure for the *m/z* 316 signal orginating from α- and β-pinene, and two possible structures resulting from α-pinene are shown in Fig. 4. These monoterpenes are generally modeled as temperature dependent emissions, and are therefore emitted at night when NO_3 chemistry is important (Sakulyanontvittaya et al., 2008). Nighttime HO_2 radical concentrations were generally 3–4 pptv (W. Brune, personal communication, 2009). Nighttime concentrations of NO_3 of 1 pptv have been predicted at the measurement site (Bouvier-Brown et al., 2009). The lifetime of α-pinene with respect to NO_3 (1 pptv) and O_3 (55 ppbv) is 220 min and 170 min, respectively, so nitrate radical chemistry is expected to compete with ozonolysis for α-pinene oxidation at night. The diurnal profile of the *m/z* 316 signal is shown in Fig. 5 as the solid line in comparison to the ISOPN nitrate signal (dashed line).

The diurnal profile of this signal peaks at night, suggesting the formation of this product from nocturnal chemistry, combined with a long atmospheric lifetime. The proposed structure for the signal at *m/z* 300 results from the photooxidation of α- or β-pinene, and has been observed in smog chamber photooxidation experiments of

α-pinene in the presence of NO_x (N. Eddingsaas, personal communication, 2009). If these four tentatively identified nitrates, and the five other unidentified nitrates listed in Table 2 are included in the comparison between the CIMS and TD-LIF, the two measurements are in close agreement, Fig. 3b.

Several of the proposed structures highlight the importance of nocturnal, nitrate radical chemistry at this rural, forested location. The formation of two of these structures requires reaction with HO_2 after reaction with NO_3. This chemistry is challenging to study in nitrate radical driven chamber experiments that can often be dominated by $RO_2 + RO_2$ reactions. Therefore, even at much lower HO_2 concentrations than encountered during peak photochemistry, HO_2 contributes to radical reactivity at night.

Another possible explanation for the unidentified organic nitrates measured by the TD-LIF instrument and not by the CIMS could be a difference in phase (gas or aerosol) of the organic nitrogen. The TD-LIF technique was operated in the field using no filter/denuder on the inlet, so the measurement should be considered the sum of gas and aerosol phase alkyl nitrates. The CIMS technique only measures the gas phase contribution to the organic nitrates. Rollins et al. (2010) have recently shown the TD-LIF technique measures both gas and aerosol phase organic nitrates, and found 15–18 % of the SOA formed from α-pinene photooxidation, initiated by OH oxidation, under high NO_x conditions was composed of alkyl nitrates. Fry et al. (2009) found 32–41 % of the aerosol mass formed in the β-pinene + NO_3 reaction was from organic nitrogen. It is possible that daytime and nocturnal oxidation of the monoterpene species at the site result in organic nitrates that partition into the aerosol phase, therefore the TD-LIF would be sensitive to the compounds and the CIMS would not. However, no aerosol organic nitrogen measurement during this campaign is available to evaluate this possibility.

4   Summary and conclusions

Observations of speciated and total alkyl and multifunctional nitrates over a ponderosa pine forest in the Sierra Nevada during the summer show total alkyl nitrates to be

composed primarily of biogenically produced nitrates. First and second generation nitrates from isoprene along with a nitrate from MBO account for two-thirds of the alkyl nitrates at the site. Based on these measurements, the organic nitrates at the site are from a mix of locally produced and transported nitrates formed from photochemical and nighttime chemistry. These measurements highlight the interaction of the Sacramento urban plume with the forested areas downwind. Similar results would be expected from other forested areas downwind of urban areas. The agreement between these two measurement techniques, TD-LIF and CIMS, supports the notion these two measurements are accurate. As areas of the tropics are developed, the impact of biogenically derived organic nitrates on ozone formation will become ever more significant.

References

Alvarado, A., Tuazon, E. C., Aschmann, S. M., Arey, J., and Atkinson, R.: Products and mechanisms of the gas-phase reactions of OH radicals and O-3 with 2-methyl-3-buten-2-ol, Atmos. Environ., 33, 2893–2905, doi:10.1016/S1352-2310(99)00106-5, 1999. 324

Aschmann, S. M., Atkinson, R., and Arey, J.: Products of reaction of OH radicals with alpha-pinene, J. Geophys. Res.-Atmos., 107, 4191, doi:10.1029/2001JD001098, 2002. 324

Atkinson, R. and Arey, J.: Gas-phase tropospheric chemistry of biogenic volatile organic compounds: a review, Atmos. Environ., 37, S197–S219, doi:10.1016/S1352-2310(03)00391-1, 2003a. 334, 343

Atkinson, R. and Arey, J.: Atmospheric degradation of volatile organic compounds, Chem. Rev., 103, 4605–4638, doi:10.1021/cr0206420, 2003b. 322

Atkinson, R., Baulch, D. L., Cox, R. A., Crowley, J. N., Hampson, R. F., Hynes, R. G., Jenkin, M. E., Rossi, M. J., Troe, J., and IUPAC Subcommittee: Evaluated kinetic and photochemical

data for atmospheric chemistry: Volume II – gas phase reactions of organic species, Atmos. Chem. Phys., 6, 3625–4055, doi:10.5194/acp-6-3625-2006, 2006. 323, 343

Barnes, I., Bastian, V., Becker, K. H., and Tong, Z.: Kinetics and products of the reactions of NO3 with monoalkenes, dialkenes, and monoterpenes, J. Phys. Chem., 94, 2413–2419, doi:10.1021/j100369a041, 1990. 325

Bouvier-Brown, N. C., Goldstein, A. H., Gilman, J. B., Kuster, W. C., and de Gouw, J. A.: In-situ ambient quantification of monoterpenes, sesquiterpenes, and related oxygenated compounds during BEARPEX 2007: implications for gas- and particle-phase chemistry, Atmos. Chem. Phys., 9, 5505–5518, doi:10.5194/acp-9-5505-2009, 2009. 334, 343

Brown, S. S., deGouw, J. A., Warneke, C., Ryerson, T. B., Dubé, W. P., Atlas, E., Weber, R. J., Peltier, R. E., Neuman, J. A., Roberts, J. M., Swanson, A., Flocke, F., McKeen, S. A., Brioude, J., Sommariva, R., Trainer, M., Fehsenfeld, F. C., and Ravishankara, A. R.: Nocturnal isoprene oxidation over the Northeast United States in summer and its impact on reactive nitrogen partitioning and secondary organic aerosol, Atmos. Chem. Phys., 9, 3027–3042, doi:10.5194/acp-9-3027-2009, 2009. 325, 334

Carter, W. P. L. and Atkinson, R.: Alkyl nitrate formation from the atmospheric photooxidation of alkanes - A revised estimation method, J. Atmos. Chem., 8, 165–173, doi:10.1007/BF00053721, 1989. 323

Chan, A. W. H., Galloway, M. M., Kwan, A. J., Chhabra, P. S., Keutsch, F. N., Wennberg, P. O., Flagan, R. C., and Seinfeld, J. H.: Photooxidation of 2-Methyl-3-Buten-2-ol (MBO) as a Potential Source of Secondary Organic Aerosol, Environ. Sci. Technol., 43, 4647–4652, doi:10.1021/es902789a, 2009. 324, 329, 343

Chen, X. H., Hulbert, D., and Shepson, P. B.: Measurement of the organic nitrate yield from OH reaction with isoprene, J. Geophys. Res.-Atmos., 103, 25563–25568, doi:10.1029/98JD01483, 1998. 323

Chuong, B. and Stevens, P. S.: Measurements of the kinetics of the OH-initiated oxidation of isoprene, J. Geophys. Res.-Atmos., 107, 4162, doi:10.1029/2001JD000865, 2002. 323

Crounse, J. D., McKinney, K. A., Kwan, A. J., and Wennberg, P. O.: Measurement of gas-phase hydroperoxides by chemical ionization mass spectrometry, Anal. Chem., 78, 6726–6732, doi:10.1021/ac0604235, 2006. 328

Crounse, J. D., Paulot, F., Kjaergaard, H. G., and Wennberg, P. O.: Peroxy radical isomerization in the oxidation of isoprene, Phys. Chem. Chem. Phys., 13, 13607–13613, doi:10.1039/c1cp21330j, 2011. 323

Day, D. A., Wooldridge, P. J., Dillon, M. B., Thornton, J. A., and Cohen, R. C.: A thermal dissociation laser-induced fluorescence instrument for in situ detection of NO2, peroxy nitrates, alkyl nitrates, and HNO_3, J. Geophys. Res.-Atmos., 107, 4046, doi:10.1029/2001JD000779, 2002. 325, 328

Day, D. A., Wooldridge, P. J., and Cohen, R. C.: Observations of the effects of temperature on atmospheric HNO_3, ΣANs, ΣPNs, and NO_x: evidence for a temperature-dependent HO_x source, Atmos. Chem. Phys., 8, 1867–1879, doi:10.5194/acp-8-1867-2008, 2008. 330

Day, D. A., Farmer, D. K., Goldstein, A. H., Wooldridge, P. J., Minejima, C., and Cohen, R. C.: Observations of NO_x, ΣPNs, ΣANs, and HNO_3 at a Rural Site in the California Sierra Nevada Mountains: summertime diurnal cycles, Atmos. Chem. Phys., 9, 4879–4896, doi:10.5194/acp-9-4879-2009, 2009. 330

Dillon, M. B., Lamanna, M. S., Schade, G. W., Goldstein, A. H., and Cohen, R. C.: Chemical evolution of the Sacramento urban plume: Transport and oxidation, J. Geophys. Res.-Atmos., 107, 4045, doi:10.1029/2001JD000969, 2002. 326

Dreyfus, G. B., Schade, G. W., and Goldstein, A. H.: Observational constraints on the contribution of isoprene oxidation to ozone production on the western slope of the Sierra Nevada, California, J. Geophys. Res.-Atmos., 107, 4365, doi:10.1029/2001JD001490, 2002. 325, 326, 343

Farmer, D. K., Perring, A. E., Wooldridge, P. J., Blake, D. R., Baker, A., Meinardi, S., Huey, L. G., Tanner, D., Vargas, O., and Cohen, R. C.: Impact of organic nitrates on urban ozone production, Atmos. Chem. Phys., 11, 4085–4094, doi:10.5194/acp-11-4085-2011, 2011. 322

Fischer, R. G., Kastler, J., and Ballschmiter, K.: Levels and pattern of alkyl nitrates, multifunctional alkyl nitrates, and halocarbons in the air over the Atlantic Ocean, J. Geophys. Res.-Atmos., 105, 14473–14494, doi:10.1029/1999JD900780, 2000. 325

Fry, J. L., Kiendler-Scharr, A., Rollins, A. W., Wooldridge, P. J., Brown, S. S., Fuchs, H., Dubé, W., Mensah, A., dal Maso, M., Tillmann, R., Dorn, H.-P., Brauers, T., and Cohen, R. C.: Organic nitrate and secondary organic aerosol yield from NO_3 oxidation of β-pinene evaluated using a gas-phase kinetics/aerosol partitioning model, Atmos. Chem. Phys., 9, 1431–1449, doi:10.5194/acp-9-1431-2009, 2009. 324, 335

Garden, A. L., Paulot, F., Crounse, J. D., Maxwell-Cameron, I. J., Wennberg, P. O., and Kjaergaard, H. G.: Calculation of conformationally weighted dipole moments useful in ion-molecule collision rate estimates, Chem. Phys. Lett., 474, 45–50, doi:10.1016/j.cplett.2009.04.038, 2009. 327

Goldstein, A. H., Hultman, N. E., Fracheboud, J. M., Bauer, M. R., Panek, J. A., Xu, M., Qi, Y., Guenther, A. B., and Baugh, W.: Effects of climate variability on the carbon dioxide, water, and sensible heat fluxes above a ponderosa pine plantation in the Sierra Nevada (CA), Agr. Forest Meteorol., 101, 113–129, doi:10.1016/S0168-1923(99)00168-9, 2000. 326

Grossenbacher, J. W., Couch, T., Shepson, P. B., Thornberry, T., Witmer-Rich, M., Carroll, M. A., Faloona, I., Tan, D., Brune, W., Ostling, K., and Bertman, S.: Measurements of isoprene nitrates above a forest canopy, J. Geophys. Res.-Atmos., 106, 24429–24438, doi:10.1029/2001JD900029, 2001. 325, 330

Grossenbacher, J. W., Barket, D. J., Shepson, P. B., Carroll, M. A., Olszyna, K., and Apel, E.: A comparison of isoprene nitrate concentrations at two forest-impacted sites, J. Geophys. Res.-Atmos., 109, D11311, doi:10.1029/2003JD003966, 2004. 325, 330

Guenther, A., Karl, T., Harley, P., Wiedinmyer, C., Palmer, P. I., and Geron, C.: Estimates of global terrestrial isoprene emissions using MEGAN (Model of Emissions of Gases and Aerosols from Nature), Atmos. Chem. Phys., 6, 3181–3210, doi:10.5194/acp-6-3181-2006, 2006. 323

Hallquist, M., Wangberg, I., Ljungstrom, E., Barnes, I., and Becker, K. H.: Aerosol and product yields from NO_3 radical-initiated oxidation of selected monoterpenes, Environ. Sci. Technol., 33, 553–559, doi:10.1021/es980292s, 1999. 322, 324

Horowitz, L. W., Fiore, A. M., Milly, G. P., Cohen, R. C., Perring, A., Wooldridge, P. J., Hess, P. G., Emmons, L. K., and Lamarque, J. F.: Observational constraints on the chemistry of isoprene nitrates over the eastern United States, J. Geophys. Res.-Atmos., 112, D12S08, doi:10.1029/2006JD007747, 2007. 323, 324, 325

Ito, A., Sillman, S., and Penner, J. E.: Effects of additional nonmethane volatile organic compounds, organic nitrates, and direct emissions of oxygenated organic species on global tropospheric chemistry, J. Geophys. Res.-Atmos., 112, D06309, doi:10.1029/2005JD006556, 2007. 322

Lamanna, M. S. and Goldstein, A. H.: In situ measurements of C-2-C-10 volatile organic compounds above a Sierra Nevada ponderosa pine plantation, J. Geophys. Res.-Atmos., 104, 21247–21262, doi:10.1029/1999JD900289, 1999. 330

Lockwood, A. L., Shepson, P. B., Fiddler, M. N., and Alaghmand, M.: Isoprene nitrates: preparation, separation, identification, yields, and atmospheric chemistry, Atmos. Chem. Phys., 10, 6169–6178, doi:10.5194/acp-10-6169-2010, 2010. 323, 324

McLafferty, F. W. and Turecek, F.: Interpretation of mass spectra, University Science Book,

Discussion Paper | Discussion Paper | Discussion Paper | Discussion Paper

Sausalito, California, 4 edn., 1993. 333

Murphy, J. G., Day, D. A., Cleary, P. A., Wooldridge, P. J., Millet, D. B., Goldstein, A. H., and Cohen, R. C.: The weekend effect within and downwind of Sacramento – Part 1: Observations of ozone, nitrogen oxides, and VOC reactivity, Atmos. Chem. Phys., 7, 5327–5339, doi:10.5194/acp-7-5327-2007, 2007. 330

Ng, N. L., Kwan, A. J., Surratt, J. D., Chan, A. W. H., Chhabra, P. S., Sorooshian, A., Pye, H. O. T., Crounse, J. D., Wennberg, P. O., Flagan, R. C., and Seinfeld, J. H.: Secondary organic aerosol (SOA) formation from reaction of isoprene with nitrate radicals (NO_3), Atmos. Chem. Phys., 8, 4117–4140, doi:10.5194/acp-8-4117-2008, 2008. 333

Noziere, B., Barnes, I., and Becker, K. H.: Product study and mechanisms of the reactions of alpha-pinene and of pinonaldehyde with OH radicals, J. Geophys. Res.-Atmos., 104, 23645–23656, doi:10.1029/1999JD900778, 1999. 324

Patchen, A. K., Pennino, M. J., Kiep, A. C., and Elrod, M. J.: Direct kinetics study of the product-forming channels of the reaction of isoprene-derived hydroxyperoxy radicals with NO, Int. J. Chem. Kinet., 39, 353–361, doi:10.1002/kin.20248, 2007. 323

Paulot, F., Crounse, J. D., Kjaergaard, H. G., Kroll, J. H., Seinfeld, J. H., and Wennberg, P. O.: Isoprene photooxidation: new insights into the production of acids and organic nitrates, Atmos. Chem. Phys., 9, 1479–1501, doi:10.5194/acp-9-1479-2009, 2009a. 323, 324, 328, 329, 334, 343

Paulot, F., Crounse, J. D., Kjaergaard, H. G., Kurten, A., St Clair, J. M., Seinfeld, J. H., and Wennberg, P. O.: Unexpected Epoxide Formation in the Gas-Phase Photooxidation of Isoprene, Science, 325, 730–733, doi:10.1126/science.1172910, 2009b. 327, 328

Paulot, F., Henze, D. K., and Wennberg, P. O.: Impact of the isoprene photochemical cascade on tropical ozone, Atmos. Chem. Phys. Discuss., 11, 25605–25654, doi:10.5194/acpd-11-25605-2011, 2011. 322

Pérez, I. M., LaFranchi, B. W., and Cohen, R. C.: Nitrogen oxide chemistry in an urban plume: investigation of the chemistry of peroxy and multifunctional organic nitrates with a Lagrangian model, Atmos. Chem. Phys. Discuss., 9, 27099–27165, doi:10.5194/acpd-9-27099-2009, 2009. 325, 332

Perring, A. E., Wisthaler, A., Graus, M., Wooldridge, P. J., Lockwood, A. L., Mielke, L. H., Shepson, P. B., Hansel, A., and Cohen, R. C.: A product study of the isoprene+NO_3 reaction, Atmos. Chem. Phys., 9, 4945–4956, doi:10.5194/acp-9-4945-2009, 2009. 323, 324

Perring, A. E., Bertram, T. H., Farmer, D. K., Wooldridge, P. J., Dibb, J., Blake, N. J., Blake, D.

R., Singh, H. B., Fuelberg, H., Diskin, G., Sachse, G., and Cohen, R. C.: The production and persistence of $\Sigma RONO_2$ in the Mexico City plume, Atmos. Chem. Phys., 10, 7215–7229, doi:10.5194/acp-10-7215-2010, 2010. 331

Rollins, A. W., Kiendler-Scharr, A., Fry, J. L., Brauers, T., Brown, S. S., Dorn, H.-P., Dubé, W. P., Fuchs, H., Mensah, A., Mentel, T. F., Rohrer, F., Tillmann, R., Wegener, R., Wooldridge, P. J., and Cohen, R. C.: Isoprene oxidation by nitrate radical: alkyl nitrate and secondary organic aerosol yields, Atmos. Chem. Phys., 9, 6685–6703, doi:10.5194/acp-9-6685-2009, 2009. 324

Rollins, A. W., Smith, J. D., Wilson, K. R., and Cohen, R. C.: Real Time In Situ Detection of Organic Nitrates in Atmospheric Aerosols, Environ. Sci. Technol., 44, 5540–5545, doi:10.1021/es100926x, 2010. 335

Rosen, R. S., Wood, E. C., Wooldridge, P. J., Thornton, J. A., Day, D. A., Kuster, W., Williams, E. J., Jobson, B. T., and Cohen, R. C.: Observations of total alkyl nitrates during Texas Air Quality Study 2000: Implications for O-3 and alkyl nitrate photochemistry, J. Geophys. Res.-Atmos., 109, D07303, doi:10.1029/2003JD004227, 2004. 331

Sakulyanontvittaya, T., Duhl, T., Wiedinmyer, C., Helmig, D., Matsunaga, S., Potosnak, M., Milford, J., and Guenther, A.: Monoterpene and sesquiterpene emission estimates for the United States, Environ. Sci. Technol., 42, 1623–1629, doi:10.1021/es800817r, 2008. 334

Saunders, S. M., Jenkin, M. E., Derwent, R. G., and Pilling, M. J.: Protocol for the development of the Master Chemical Mechanism, MCM v3 (Part A): tropospheric degradation of non-aromatic volatile organic compounds, Atmos. Chem. Phys., 3, 161–180, doi:10.5194/acp-3-161-2003, 2003. 324, 331, 343

Schade, G. W., Goldstein, A. H., Gray, D. W., and Lerdau, M. T.: Canopy and leaf level 2-methyl-3-buten-2-ol fluxes from a ponderosa pine plantation, Atmos. Environ., 34, 3535–3544, doi:10.1016/S1352-2310(00)00120-5, 2000. 330

Spencer, K. M., Beaver, M. R., Clair, J. M. St., Crounse, J. D., Paulot, F., and Wennberg, P. O.: Quantification of hydroxyacetone and glycolaldehyde using chemical ionization mass spectrometry, Atmos. Chem. Phys. Discuss., 11, 23619–23653, doi:10.5194/acpd-11-23619-2011, 2011. 327

Sprengnether, M., Demerjian, K. L., Donahue, N. M., and Anderson, J. G.: Product analysis of the OH oxidation of isoprene and 1,3-butadiene in the presence of NO, J. Geophys. Res.-Atmos., 107, 4269, doi:10.1029/2001JD000716, 2002. 323

St. Clair, J. M., McCabe, D. C., Crounse, J. D., Steiner, U., and Wennberg, P. O.: Chemical ion-

ization tandem mass spectrometer for the in situ measurement of methyl hydrogen peroxide, Rev. Sci. Instrum., 81, 094102, doi:10.1063/1.3480552, 2010. 326, 327, 328

Starn, T. K., Shepson, P. B., Bertman, S. B., Riemer, D. D., Zika, R. G., and Olszyna, K.: Nighttime isoprene chemistry at an urban-impacted forest site, J. Geophys. Res.-Atmos., 103, 22437–22447, doi:10.1029/98JD01201, 1998. 334

Su, T. and Chesnavich, W. J.: Parameterization of the ion-polar molecule collision rate-constant by trajectory calculations, J. Chem. Phys., 76, 5183–5185, doi:10.1063/1.442828, 1982. 327

Tuazon, E. C. and Atkinson, R.: A product study of the gas-phase reaction of isoprene with the OH radical in the prescence of NO_x, Int. J. Chem. Kinet., 22, 1221–1236, doi:10.1002/kin.550221202, 1990. 323

Wolfe, G. M., Thornton, J. A., Bouvier-Brown, N. C., Goldstein, A. H., Park, J.-H., McKay, M., Matross, D. M., Mao, J., Brune, W. H., LaFranchi, B. W., Browne, E. C., Min, K.-E., Wooldridge, P. J., Cohen, R. C., Crounse, J. D., Faloona, I. C., Gilman, J. B., Kuster, W. C., de Gouw, J. A., Huisman, A., and Keutsch, F. N.: The Chemistry of Atmosphere-Forest Exchange (CAFE) Model – Part 2: Application to BEARPEX-2007 observations, Atmos. Chem. Phys., 11, 1269–1294, doi:10.5194/acp-11-1269-2011, 2011. 343

Wu, S. L., Mickley, L. J., Jacob, D. J., Logan, J. A., Yantosca, R. M., and Rind, D.: Why are there large differences between models in global budgets of tropospheric ozone?, J. Geophys. Res.-Atmos., 112, D05302, doi:10.1029/2006JD007801, 2007. 322, 323

Table 1. Locally observed and estimated alkyl nitrate VOC precursors for BEARPEX 2009. Mixing ratios (MR) are mean afternoon (12:00–18:00 PST) concentrations. Nitrate yields and rate constants are from the literature as cited.

VOC	MR (ppb)	α	$k_{\mathrm{OH+VOC}}$	P_{ANs}(ppb h^{-1})[f]	fracP$_{\mathrm{ANs}}$(calc)
ANs	0.5	0.15	5.0×10^{-11}[a]	0.08	0.07
benzene	0.029	0.03[g]	1.2×10^{-12}[b]	0.0	0.0
toluene	0.128	0.08[g]	6.21×10^{-12}[b]	0.0	0.0
isoprene	1.91	0.10[g]	1.0×10^{-10}[b]	0.41	0.36
MVK	1.11	0.01[g]	2.0×10^{-11}[c]	0.0	0.0
MACR	0.43	0.0[g]	2.9×10^{-11}[c]	0.0	0.0
β-pinene	0.116	0.2[g]	7.7×10^{-11}[d]	0.04	0.03
α-pinene	0.152	0.2[g]	5.3×10^{-11}[c]	0.03	0.03
MBO	4.45	0.10[h]	5.8×10^{-11}[d]	0.56	0.49
camphene	0.018	0.2[i]	5.3×10^{-11}[d]	0.0	0.0
methane	1800[e]	0.001[g]	6.4×10^{-15}[c]	0.0	0.0
TOTAL				1.14	

[a] Paulot et al. (2009a); [b] Atkinson and Arey (2003a); [c] Atkinson et al. (2006); [d] Atkinson and Arey (2003a); [e] estimated; [f] OH = 6 × 10^6 molecules cm^{-3} (Bouvier-Brown et al., 2009; Wolfe et al., 2011; Dreyfus et al., 2002); [g] MCMv3.2 (Saunders et al., 2003); [h] Chan et al. (2009); [i] assumed to have the same yield as the pinenes.

Table 2. Significant nitrogen-containing *m/z* observed with the CIMS. The *m/z* column indicates the signal in the mass spectrum. The m.w. column is the inferred molecular weight (*m/z* −85).

m/z	m.w.	max MR (ppt)	proposed structure
220	135	10	–
230	145	28	a
236	151	5	–
244	159	30	–
246	161	11	–
248	163	44	b
262	177	16	–
300	215	30	c
316	231	44	d
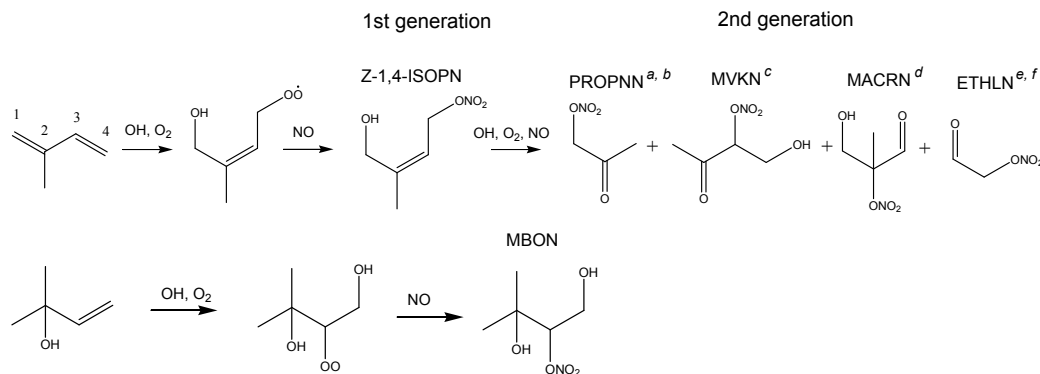
Fig. 1. Organic nitrates from isoprene and MBO photooxidation observed in this study. Only one isoprene hydroxynitrate from the eight possible isoprene nitrate isomers is shown here. Only ETHLN forms from the isoprene hydroxynitrate isomer shown here. The other second generation nitrates can form from the isomers indicated by the superscripted letters (a: 4,1-ISOPN; b: 2,1-ISOPN; c: 4,3-ISOPN; d: 1,2-ISOPN; e: 3,4-ISOPN; f: 1,4-ISOPN, shown).
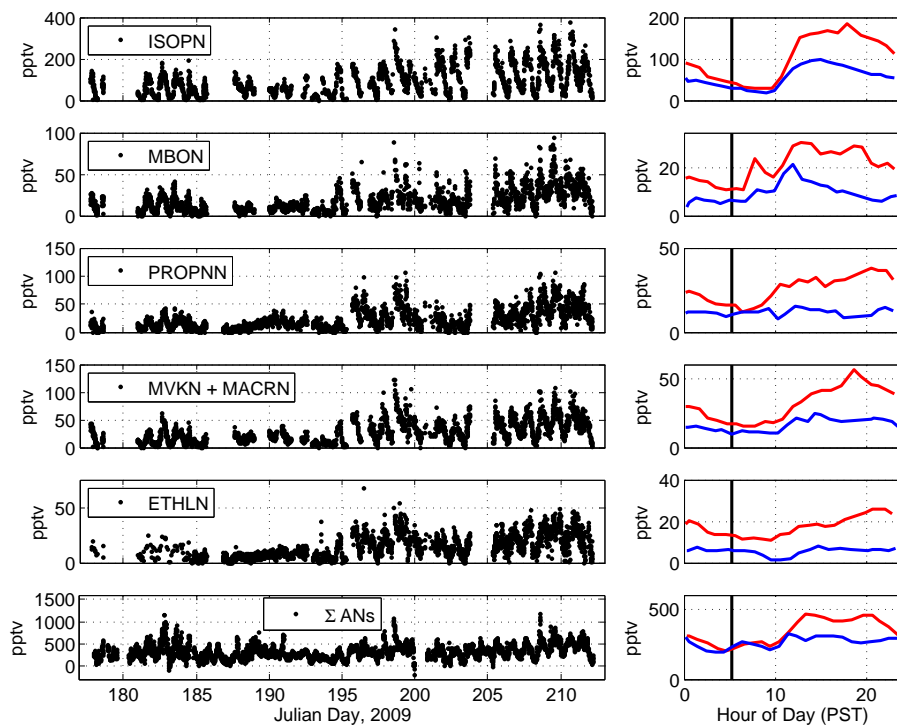
Fig. 2. Time series (left) and mean diurnal profiles (right) of organic nitrates and ΣANs measured during BEARPEX 2009. Diurnal profiles shown in red are mean concentrations on days with maximum daytime temperatures of 26 ˚C and higher. Blue diurnal profile is the mean concentration on days with maximum temperatures less than 26 ˚C. Vertical lines indicate local sunrise.

Full Screen / Esc

Printer-friendly Version

Interactive Discussion

Fig. 3. (a) Comparison of CIMS and TD-LIF measurements during the last two weeks of the campaign (Julian days 199–212). ΣANs as measured by TD-LIF are shown as the dashed line. Speciated organic nitrates are shown in the colors. The gray fraction represents the sum of other organic nitrate species observed with the CIMS (Table 2). Red = ISOPN, Green = PROPNN, Black = MVKN + MACRN, Magenta = MBON, Blue = ETHLN. **(b)** In blue, ΣANs (measured with TD-LIF) vs. the sum of individual nitrates (measured with CIMS), not including the data in the gray portion. Equation for the linear fit is $y = 1.25x + 0.096$, $R^2 = 0.85$. In red, ΣANs (measured with TD-LIF) vs. the sum of individual nitrates (measured with CIMS), including the data in the gray portion. Equation for the linear fit is $y = 0.91x + 0.052$, $R^2 = 0.89$. There are fewer data points for the data shown in red due to the frequency of data points (approximately once every 1.6 h).
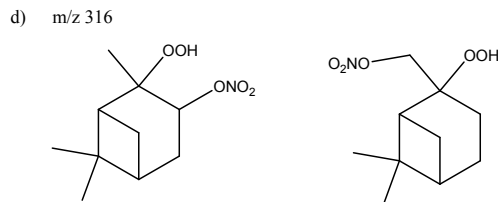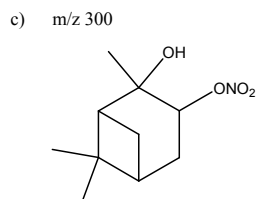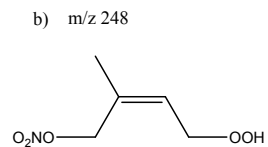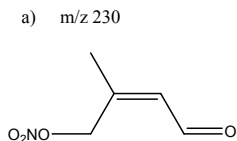
a) m/z 230

b) m/z 248

c) m/z 300

d) m/z 316

Fig. 4. Proposed structures for even mass signals listed in Table 2. *m/z* 248 could also be due to MBO + NO₃ chemistry, but since the NO₃ rate constant is ~500 times lower than with *α*-pinene, and ~60 times lower than isoprene, it is expected to be a minimal contribution.
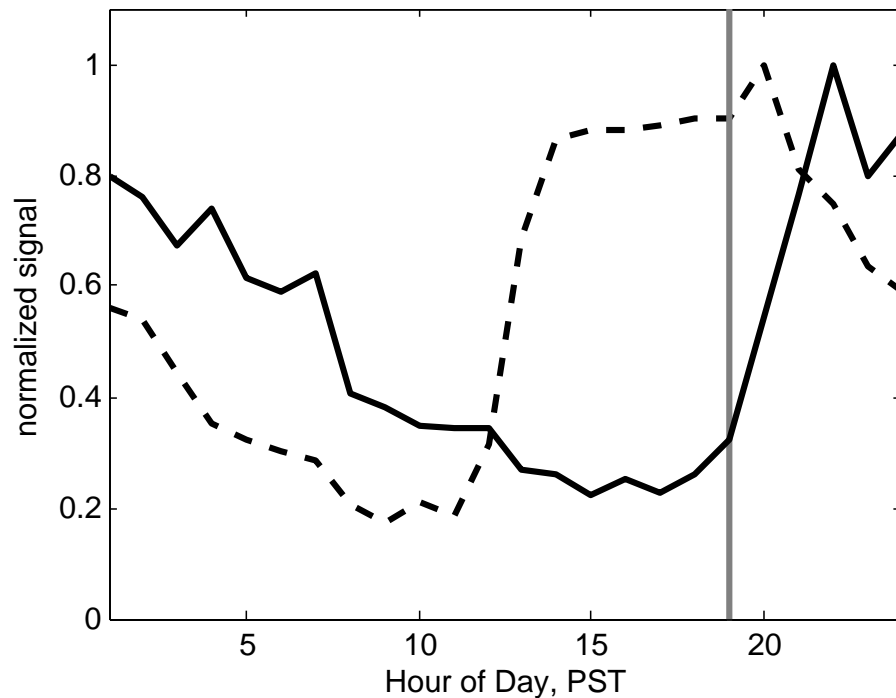
Fig. 5. Average, normalized diurnal signal of the *m/z* 316 product, proposed as the nitrooxy-hydroperoxide from α-pinene (solid line). The concentration of this species peaks at night, in contast with the ISOPN signal shown as the dashed line. The solid gray line indicates the approximate time of local sunset.